PAPER

Check for updates

A biocompatible poly(amidoamine) (PAMAM) dendrimer octa-substituted with α-cyclodextrin towards the controlled release of doxorubicin hydrochloride from its ferrocenyl prodrug†

Artur Kasprzak, (ID) * Bartłomiej Dabrowski and Agnieszka Zuchowska (ID)

Facile and efficient methods for the synthesis of the first poly(aminodamine) PAMAM G1.0 dendrimer octa-substituted with α-cyclodextrin and a novel ferrocenyl prodrug of doxorubicin hydrochloride are developed. This vector is non-toxic and can bind the designed ferrocenyl prodrug. It also shows a controlled drug release profile and high cytotoxicity against breast cancer cells (MCF-7), as elucidated by the *in vitro* biological studies performed with an innovative cell-on-a-chip microfluidic system.

Poly(amidoamine) (PAMAM) dendrimers are of the highest interest to general medicinal chemistry.[1–3] These dendrimers show beneficial physicochemical or biological properties in comparison with the respective polyamine polymers, *e.g.*, polyethylenimine (PEI). In general, the cytotoxicity of PAMAM dendrimers is lower in comparison to that of PEI, which is an important factor in terms of the development of non-viral drugs or gene delivery vectors. The unique shape of PAMAM dendrimers as well as the presence of highly reactive amino groups imply interesting possibilities towards the construction of novel systems dedicated to modern therapies in humans.

In recent years, the chemistry and application of PAMAM dendrimer nanoconjugates with cyclodextrins (CDs) has drawn an unflagging interest.[4–7] CDs are the supramolecules formed of six, seven or eight D-glucose units, which are coupled *via* α-1,4-glycosidic bonds.[8,9] CDs form cup-shaped molecules. Their cavity is hydrophobic, whilst the exterior is hydrophilic. As a result, CDs show unique properties towards the formation of host–guest complexes with hydrophobic compounds, including drugs.[10–12] From the point of view of applied medicinal chemistry, the presence of CDs in the therapeutic system provides the possibility to release a drug in a controlled way. It is associated with the strategy of stepwise release of a drug from the inner cavity of CD. Furthermore, CDs increase the water solubility and/or biocompatibility of the drug delivery vector. The above-mentioned features make CDs promising candidates for the decoration of PAMAM dendrimers. PAMAM dendrimers grafted with CD moieties can be used as versatile delivery agents. The

uses of such macromolecular species cover the binding and release of various therapeutic species, including nucleic acids (*e.g.*, siRNA or DNA)[13–16] or drugs (*e.g.*, doxorubicin or sodium methotrexate).[6,17,18] These dendrimeric structures showed encouraging biological properties towards their use in medicinal chemistry, especially in terms of the design of novel anti-cancer agents. In some cases, additional structural motifs were introduced to these vectors, such as poly(ethylene glycol) (PEG) residues, towards providing specific biological or physico-chemical properties.[18,19] The studies dealing with the application of PAMAM-CD architectures towards the construction of biosensors were also reported.[20,21] Furthermore, interesting studies on the solubilisation of highly hydrophobic fullerenes with PAMAM-CD-PEG vectors[19] or cobaltocene-bridged PAMAM-CD dendrimers were also reported. These examples clearly elucidate the capabilities of PAMAM-CD nanoconjugates towards their use in modern applied chemistry, including nanomedicine.

The use of ferrocene (Fc) in medicinal chemistry has been studied over the years.[22–31] Some of the reports deal with the synthesis of Fc-templated drugs[23,24] or prodrugs.[25–31] The latter concept is especially interesting from the point of view of applied medicinal chemistry, since prodrug technology may improve the biocompatibility and/or bioaccessibility of a drug.[32–34] However, the reports dealing with the formation of Fc-based prodrugs are still sparse; they cover, *e.g.*, the synthesis of Fc-functionalized nucleobases[31] or synthesis and biological evaluation of the prodrugs bearing Fc and boronic acid moieties.[25,26] Interestingly, Fc is known for the formation of stable host–guest inclusion complexes with CD.[27,28] Fc is not soluble in water, thus, it is not released from its complex with CD in an aqueous medium. Fc release can be only achieved *via* a redox process (ferrocenyl cation does not form stable inclusion complexes) and the employment of this concept can be indeed

Faculty of Chemistry, Warsaw University of Technology, Noakowskiego Str. 3, 00-664 Warsaw, Poland. E-mail: akasprzak@ch.pw.edu.pl

found in the literature.[29,30] Thus, Fc can also be employed as the building block for macromolecular therapeutic systems, including self-assembling drug delivery systems.[35–38] An interesting example is the formation of a pH-responsive supramolecular system for controlled drug release, which is based on the self-assembly of the Fc-PEG conjugate and β-cyclodextrin-functionalized doxorubicin hydrochloride.[35] The drug in this system, that is doxorubicin hydrochloride (DOX*HCl), was released by means of an oxidant-dependent process. This system showed promising biological features towards cancer treatments. In fact, DOX*HCl is commonly the first and/or best choice drug for the treatment of various cancers, including breast or lung cancer.[39–41]

In pursuit of the design of novel anticancer agents, herein, we present efficient and facile methods for the preparation of the first PAMAM G1.0 dendrimer octa-substituted with α-cyclodextrin (octa-αCD-PAMAM) and a novel DOX*HCl prodrug, namely ferrocenyl ester of doxorubicin hydrochloride (Fc–COO–DOX*HCl). Octa-αCD-PAMAM is non-toxic and has the property to bind Fc–COO–DOX*HCl. The *in vitro* studies revealed encouraging biological features of the designed nanoconjugate, namely controlled drug release behavior and high cytotoxicity against breast cancer cell line (MCF-7). *In vitro* biological assays were performed with an innovative cell-on-a-chip microfluidic system. We anticipate our findings will further stimulate the progress in medicinal chemistry with the use of macromolecular therapeutic systems exhibiting a controlled drug release profile.

The procedure for the synthesis of octa-αCD-PAMAM (3) is presented in Fig. 1. In general, this derivative of PAMAM G1.0 (1) was obtained in good yield (80%) by means of a reductive amination approach with the use of α-cyclodextrin mono-aldehyde (αCD-CHO; 2). The reaction occurred between each of the eight terminals, primary amino groups of 1, and formyl

moieties of 2. In the first step of the reaction, imine-bonds were formed and then they were reduced to CH_2NH_2 linkages by means of the treatment with sodium triacetoxyborohydride.[42] The obtained octa-αCD-PAMAM (3) was characterized with NMR and FT-IR spectroscopies, as well as with ESI-MS.[43] It is noteworthy that elemental analysis and ESI-MS experiment ultimately confirmed the introduction of eight αCD residues to one molecule of PAMAM G1.0; the calculated and found data were highly consistent. It means that the herein developed methodology enables the full functionalization of PAMAM's terminal amino groups with biocompatible, αCD residues.

The ferrocenyl ester of DOX*HCl (Fc–COO–DOX*HCl; 5) was obtained by means of the treatment of DOX*HCl with ferrocenecarboxylic acid (Fc-COOH; 4). The synthetic scheme is presented in Fig. 2. This process was based on the carbodiimide-mediated ester bond formation reaction (Steglich esterification) with the inclusion of a carboxyl group of 4 and the terminal CH_2OH moiety of DOX*HCl.[42] It is worth noting that no reaction occurred between the amino group of DOX*HCl since this moiety remained in the form of hydrochloride during all the reaction and purification steps (no alkaline conditions were applied in our synthesis). Thus, in our methodology native DOX*HCl can be used, without the need for amino group protection[44] or use of enzymatic process.[45] Combination of NMR
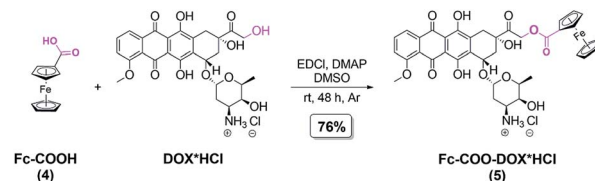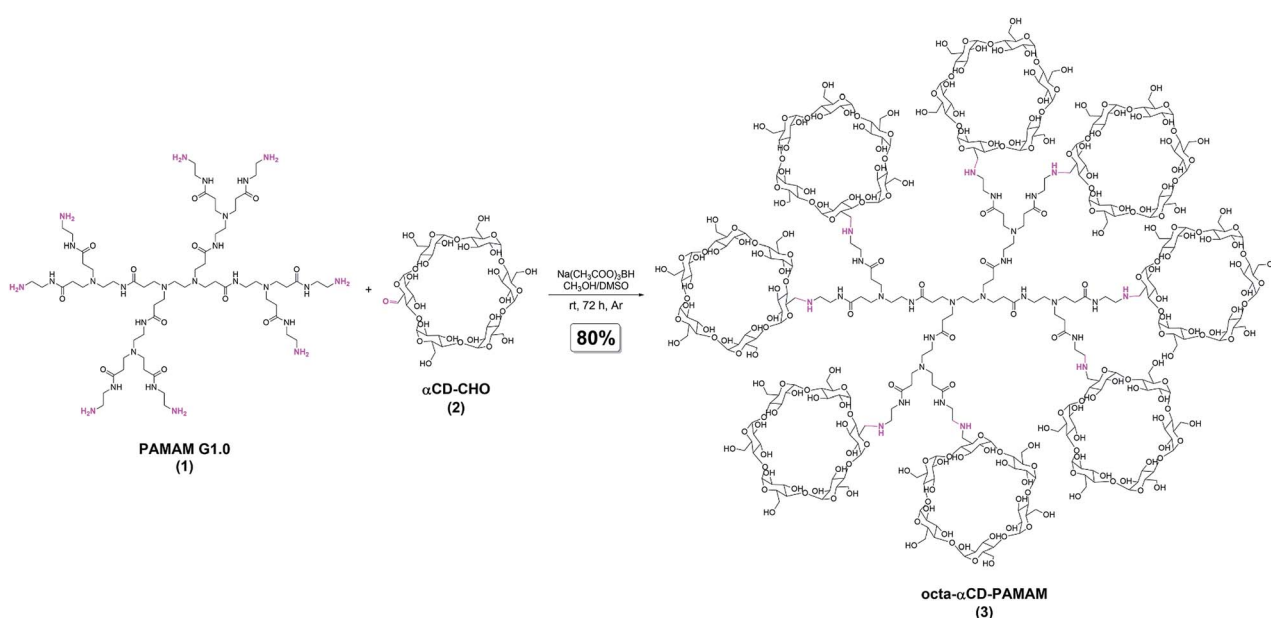

Fig. 2 Synthesis of Fc–COO–DOX*HCl (5).

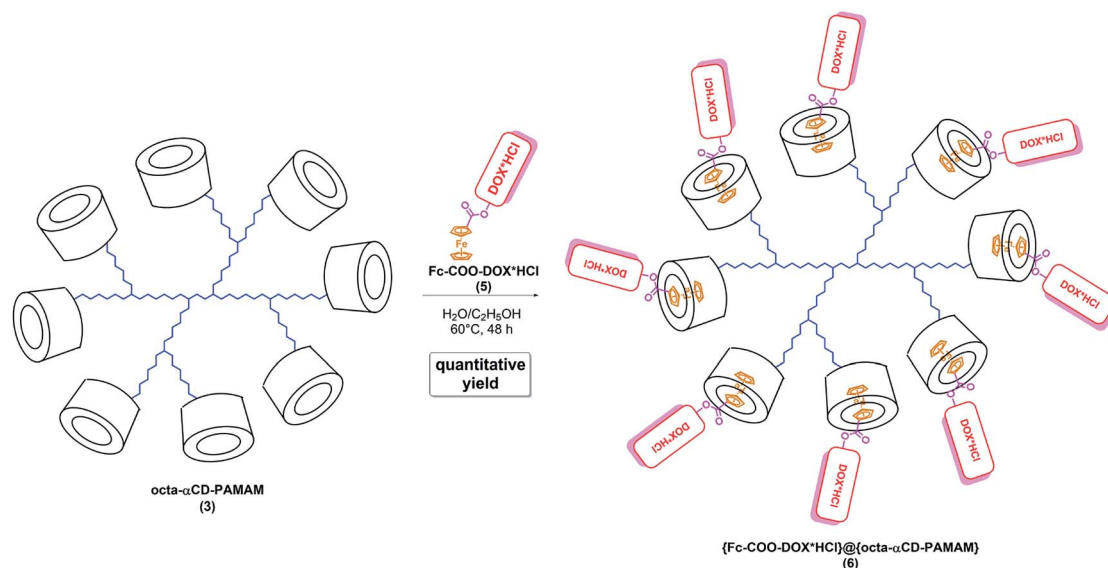**Fig. 1** Synthesis of octa-αCD-PAMAM (3).

Fig. 3 Synthesis of Fc−COO−DOX*HCl (**5**). For the structures of **3** and **5**, see Fig. 1 and 2.

and FT-IR spectroscopies, as well as high-resolution mass spectrometry (HRMS) confirmed the formation of pure Fc–COO–DOX*HCl (**5**), a novel DOX*HCl prodrug, which bears the ferrocenyl moiety.[43]

With both octa-αCD-PAMAM (**3**) and Fc–COO–DOX*HCl (**5**) at hand, we began to merge their chemistries (Fig. 3). Our concept originated from the following facts. Fc is known for its capability to form very stable complexes with αCD.[27,28] αCD can accommodate one Fc residue, since the width of the inner cavity of αCD equals to 5.7 Å, whilst its depth is 7.8 Å. On the other hand, DOX*HCl molecule is too big to be effectively complexed inside the inner cavity of αCD; for this purpose, a larger CD should be used, such as β-cyclodextrin (width of inner cavity 7.8 Å) or γ-cyclodextrin (width of inner cavity 8.8 Å).[46–48] Therefore, in our system, Fc-mediated complexation with Fc–COO–DOX*HCl (**5**) and αCD units of octa-αCD-PAMAM (**3**) occurs. We have successfully obtained the desired nanoconjugate {Fc–COO–DOX*HCl}@{octa-αCD-PAMAM} (**6**) in quantitative yields using a combination of solution and lyophilisation methodology.[42] FT-IR spectroscopy suggested the anticipated Fc-oriented complexation for this nanoconjugate, since no absorption bands coming from Fc moiety of **5** were observed in the spectrum of nanoconjugate **6**, whilst absorption bands coming from DOX*HCl were found.[49] Importantly, ESI-MS and elemental analysis confirmed the formation of the desired nanoconjugate **6**; the calculated and obtained data were highly consistent.[43] Additionally, we further studied the complex formation phenomenon with NMR techniques. At first, the Fc-oriented complexation was tracked with ^{1}H–^{1}H ROESY NMR.[25] The ^{1}H–^{1}H ROESY NMR spectrum of **6** featured the cross-correlations between Fc's cyclopentadienyl signals (H_{Cp}) and H-3, H-5 inner protons of α-CD (Fig. 4). It was ascribed to the inclusion of Fc inside α-CD's inner cavity. It stands for the successful formation of inclusion complexes between guest **5** and α-CD units of **3**. Secondly, the results of ^{1}H DOSY NMR

analysis suggested the formation of a single host–guest system. ^{1}H DOSY NMR technique involves the measurement of the diffusion coefficient of the compounds forming a sample and is a powerful and versatile NMR method for the analyses of the
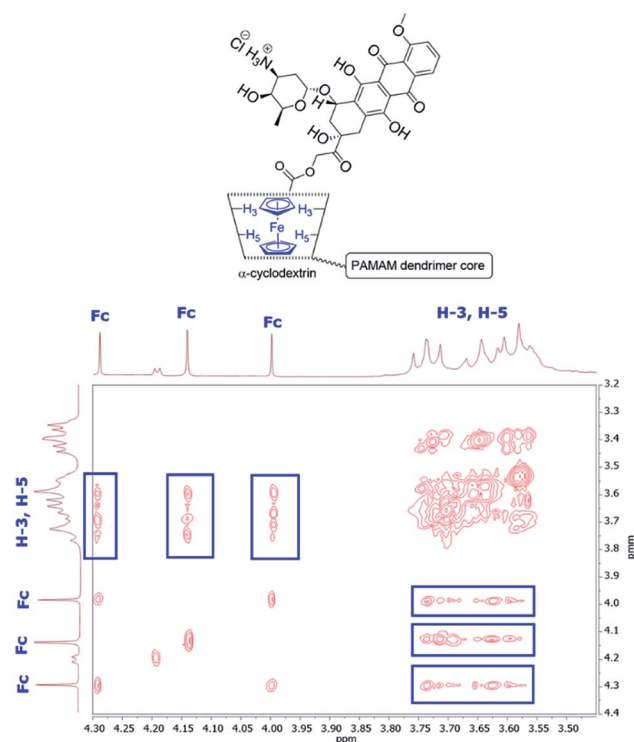

Fig. 4 The 4.30−3.45 ppm inset of the [1]H−^{1}H ROESY NMR (DMSO-d_6: D$_2$O = 1 : 1 v/v, 500 MHz) spectrum of nanoconjugate {Fc−COO−DOX*HCl}@{octa-αCD-PAMAM} (**6**) presenting the crucial cross-correlations standing for the inclusion phenomenon (these cross-correlations are marked in blue). The graphical representation of the complex is also shown.

supramolecular systems, including host-guest complexes.[25,50,51] The ¹H DOSY NMR spectrum of nanoconjugate **6** showed one diffusion coefficient value (0.358 10⁻¹⁰ m² s⁻¹).[52b] Thus, we hypothesized that a single host-guest system might have been formed. In other words, we claim that neither unbound **5** nor other dendrimeric structures (*i.e.*, bearing less than eight complexed molecules of **5**) were found in the sample. To further support this hypothesis, ¹H DOSY NMR spectra in the same solvent were acquired for native host **3** and guest **5**.[52a] Both of these showed higher diffusion coefficient values than the resultant nanoconjugate **6**. As expected, the diffusion coefficient value for **5** (3.699 10⁻¹⁰ m² s⁻¹) was found to be higher than that for **3** (0.746 10⁻¹⁰ m² s⁻¹; this is because **3** is much bigger than **5**). This clear difference in the diffusion coefficient values between the molecules forming the system (**3**, **5**) and their resultant inclusion complex **6** support our claim on the host–guest chemistry behaviour for the studied system.[52] Finally, UV-Vis spectroscopy was applied to provide an insight into the stoichiometry of the host-guest complexes of **3** and **5**.[25] The UV-Vis spectra of guest **5** featured an increase in the absorbance in the presence of host **3**, as well as some slight blue shift behaviour.[52b] These features were ascribed to the inclusion phenomenon. This change differed between the samples that enabled the estimation of complex stoichiometry. The complex stoichiometry was estimated on the basis of Job's plot analysis.[25] The estimated stoichiometry was found to be 1 : 8 (host : guest);[52b] this conclusion supported the outcomes from the ESI-MS experiment and is highly consistent with other above-presented supramolecular analyses. All these important features mentioned above mean that the herein developed methodology enables full "blocking" of αCD's cavities with ferrocenyl units of DOX*HCl prodrug **5** by means of the formation of Fc-oriented complexes.

We envision that DOX*HCl might be released from nanoconjugate **6** under acidic conditions. Our hypothesis was based on two facts. Firstly, DOX*HCl is bound to this nanoconjugate in the form of its ferrocenyl prodrug (ester bond) by means of Fc-oriented complexation. Ester bonds are known for their prospective use in prodrug technologies.[32–34] Secondly, the pH of cancer cells was found to be acidic (pH 4–6).[53–55] It gives the possibility of a controlled drug release at the therapeutic target (cancer cell environment). In order to examine the possibility of DOX*HCl release from nanoconjugate **6** and the profile of this release, *in vitro* controlled drug release trials at pH 4.7 were performed.[56] The DOX*HCl release curve is presented in Fig. 5a, blue curve. This curve resembles the characteristic controlled drug release profile. It means that DOX*HCl release from nanoconjugate **6** was stepwise. This controlled release was ascribed to the hydrolysis of ester bonds between Fc and DOX*HCl parts of compound **5** complexed inside αCD units within nanoconjugate **6**. The cumulative release of DOX*HCl after 24 hours equalled to *ca.* 78% and the final cumulative release (after 72 hours) was found to be *ca.* 87%. The first, relatively fast, DOX*HCl release segment up to *ca.* 12 h was ascribed to the release of DOX*HCl molecules that were close to the dendrimer–buffer interface.[57] Subsequently, the cumulative release of DOX*HCl increased gradually with the contact time.
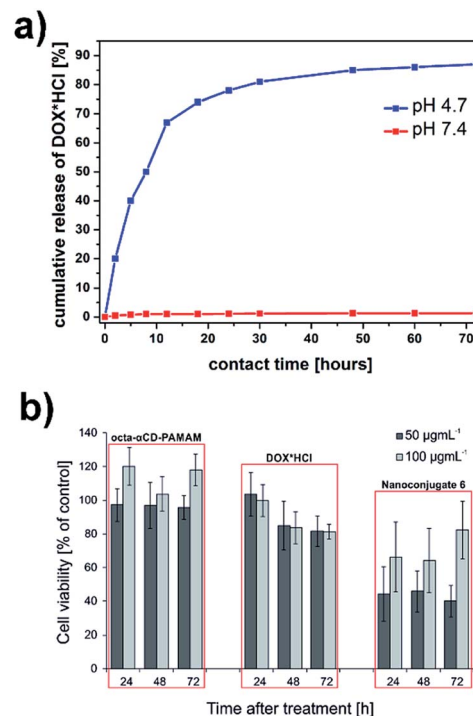

Fig. 5 (a) DOX*HCl release curves from nanoconjugate **6** at pH 4.7 and pH 7.4; (b) MCF-7 cell viability after treatment during long-term spheroid culture.

The plateau segment was achieved between 48 h and 72 h. This high total cumulative release value at a rationally short time constitutes a good starting point for the design of novel macromolecular therapeutics exhibiting a controlled drug release profile. For comparison, drug release trials were also performed at pH 7.4 (physiological pH; Fig. 5a, red curve). No significant drug release was found in this environment (cumulative DOX release was lower than *ca.* 1.5%, which means that in practise no compound, neither **5** nor any of its subpart (*e.g.*, DOX), was released from **6**). This finding means that (i) for our system simple equilibrium displacement during the dialysis did not take place, which confirms that the release of the drug is driven by acidic pH (hydrolysis of an ester bond), (ii) no unbound **5** was present in nanoconjugate **6**.

Encouraged by the above-presented results, we estimated the cytotoxicity profile of the designed nanoconjugate **6** against breast cancer (MCF-7) spheroids. These studies were performed using an innovative cell-on-a-chip microfluidic system. Cell-on-a-chip are miniature, microfluidic devices that contain *in vitro* cell cultures under flow conditions that simulate physiology at the tissue level.[58] Unlike conventional *in vitro* cell culture methods, microfluidic-based cell cultures to a greater extent reproduce the *in vivo* conditions. It is associated with the combination of surfaces mimicking extracellular matrix geometries and microfluidic channels that regulate fluid transport (nutrients important for cells).[59] In our research, we used the innovative microfluidic device for long-term three-dimensional (3D) spheroid cell culture.[60] The use of three-dimensional cell contact and the flow conditions in a single device allowed more

than standard two-dimensional cell cultures to reproduce the *in vivo* environment of breast cancer. Moreover, this device allowed us to perform quick and precise microscopic and fluorescence analysis after the drug treatment. The microscopic analysis involved the observation of morphological spheroid changes (in single, always the same spheroid) while fluorescence analysis involved the evaluation of the metabolic activity of spheroids (their viability). The results of biological assays are shown in Fig. 5b.[61] At first, the cytotoxicity profile of octa-αCD-PAMAM (3) was estimated. This dendrimeric vector in each tested concentration was found to be non-toxic, which is beneficial in terms of its use as a drug delivery vector. The same situation was observed with free DOX*HCl. On the other hand, nanoconjugate 6 showed different cytotoxicity profiles; nanoconjugate 6 was found to be highly toxic to breast cancer cells. Cell viability after 72 h equated to *ca.* 40%. In comparison, this viability for octa-αCD-PAMAM (3) and free DOX*HCl (50 µg mL^{-1}, 72 h) was *ca.* 95% and *ca.* 81%, respectively. During our studies, we also observed that higher concentrations of the tested substances were less toxic to breast cancer cells. This can be related to the defense mechanism of cancer tumors; cancer tumors recognize higher concentrations of toxic substances and do not absorb them from the external environment.[62] In addition, higher cell viability may be associated with the stimulation of cell proliferation after using higher concentrations of octa-αCD-PAMAM. We observed that the free drug carrier at higher concentrations increases the viability of MCF-7 cells (Fig. 5b). Similarly, the MCF-7 viability after treatment with a higher concentration of nanoconjugate 6 was also higher.

Conclusions

In conclusion, we present an efficient and facile method for the synthesis of the first PAMAM G1.0 dendrimer octa-substituted with αCD (octa-αCD-PAMAM), as well as its application for binding the newly synthesized ferrocenyl ester of DOX*HCl (Fc–COO–DOX*HCl). The release profile of DOX*HCl from the designed nanoconjugate at pH 4.7 resembled the characteristic controlled drug release curve. Dendrimeric octa-αCD-PAMAM is biocompatible and non-toxic, whilst its nanoconjugate with Fc–COO–DOX*HCl is highly toxic against breast cancer cells (MCF-7; the biological assays were performed with an innovative cell-on-a-chip microfluidic system). This manuscript sheds light on the design of new therapeutic, macromolecular systems featuring a controlled drug release profile, opening new avenues in medicinal chemistry.

Conflicts of interest

There are no conflicts to declare.

Acknowledgements

Notes and references

1 M. A. Mintzer and M. W. Grinstaff, *Chem. Soc. Rev.*, 2011, **40**, 173–190.

2 R. K. Tekade, P. V. Kumar and N. K. Jain, *Chem. Rev.*, 2009, **109**, 49–87.

3 D. Astruc, E. Boisselier and C. Ornelas, *Chem. Rev.*, 2010, **110**, 1857–1959.

4 N. Li, X. Wei, Z. Mei, X. Xiong, S. Chen, M. Ye and S. Ding, *Carbohydr. Res.*, 2011, **346**, 1721–1727.

5 F. Kihara, H. Arima, T. Tsutsumi, F. Hirayama and K. Uekama, *Bioconjugate Chem.*, 2003, **14**, 342–350.

6 Y. Huang and Q. Kang, *J. Inclusion Phenom. Macrocyclic Chem.*, 2012, **72**, 55–61.

7 G. R. Newkome and C. D. Shreiner, *Polymer*, 2008, **49**, 11–73.

8 G. Crini, *Chem. Rev.*, 2014, **114**, 10940–10975.

9 E. M. M. Del Valle, *Process Biochem.*, 2004, **39**, 1033–1046.

10 A. L. Laza-Knoerr, R. Gref and P. Couvreur, *J. Drug Target.*, 2010, **18**, 645–656.

11 V. Bonnet, C. Gervaise, F. Djedaini-Pilard, A. Furlan and C. Sarazin, *Drug Discov. Today*, 2015, **20**, 1120–1126.

12 A. Kasprzak and M. Poplawska, *Chem. Commun.*, 2018, **54**, 8547–8562.

13 H. Arima, F. Kihara, F. Hirayama and K. Uekama, *Bioconjugate Chem.*, 2001, **12**, 476–484.

14 A. F. Abdelwahab, A. Ohyama, T. Higashi, K. Motoyama, K. A. Khaled, H. A. Sarhan, A. K. Hussein and H. Arima, *J. Drug Target.*, 2014, **22**, 927–934.

15 H. Arima, K. Motoyama and T. Higashi, *Pharmaceutics*, 2012, **4**, 130–148.

16 H. Arima and K. Motoyama, *Sensors*, 2009, **9**, 6346–6361.

17 H. Wang, N. Shao, S. Qiao and Y. Cheng, *J. Phys. Chem. B*, 2012, **116**, 11217–11224.

18 M. Saraswathy, G. T. Knight, S. Pilla, R. S. Ashton and S. Gong, *Colloids Surf., B*, 2015, **126**, 590–597.

19 C. Kojima, Y. Toi, A. Harada and K. Kono, *Bioconjugate Chem.*, 2008, **19**, 2280–2284.

20 R. Villalonga, P. Díez, M. Gamella, A. J. Reviejo, S. Romano and J. M. Pingarrón, *Electrochim. Acta*, 2012, **76**, 249–255.

21 B. González, C. M. Casado, B. Alonso, I. Cuadrado, M. Morán, Y. Wang and A. E. Kaifer, *Chem. Commun.*, 1998, 2569–2570.

22 C. Ornelas, *New J. Chem.*, 2011, **35**, 1973–1985.

23 O. Buriez, J. M. Heldt, E. Labb, A. Vessieres, G. Jaouen and C. Amatore, *Chem.–Eur. J.*, 2008, **14**, 8195–8203.

24 Z. Petrovski, M. R. P. Norton de Matos, S. S. Braga, C. C. L. Pereira, M. L. Matos, I. l S. Goncalves, M. Pillinger, P. M. Alves and C. C. Romao, *J. Organomet. Chem.*, 2008, **693**, 675–684.

25 A. Kasprzak, M. Koszytkowska-Stawińska, A. M. Nowicka, W. Buchowicz and M. Poplawska, *J. Org. Chem.*, 2019, **84**, 15900–15914.

26 H. Hagen, P. Marzenell, E. Jentzsch, F. Wenz, M. R. Veldwijk and A. Mokhir, *J. Med. Chem.*, 2012, **55**, 924–934.

27 F. Hapiot, S. Tilloy and E. Monflier, *Chem. Rev.*, 2006, **106**, 767–781.

28 J.-S. Wu, K. Toda, A. Tanaka and I. Sanemasa, *Bull. Chem. Soc. Jpn.*, 1998, **71**, 1615–1618.

29 M. Nakahata, Y. Takashima, H. Yamaguchi and A. Harada, *Nat. Commun.*, 2011, **2**, 511.

30 F. Szillat, B. V. K. J. Schmidt, A. Hubert, C. Barner-Kowollik and H. Ritter, *Macromol. Rapid Commun.*, 2014, **35**, 1293–1300.

31 S. Daum, V. F. Chekhun, I. N. Todor, N. Y. Lukianova, Y. V. Shvets, L. Sellner, K. Putzker, J. Lewis, T. Zenz, I. A. M. de Graaf, G. M. M. Groothuis, A. Casini, O. Zozulia, F. Hampel and A. Mokhir, *J. Med. Chem.*, 2015, **58**, 2015–2024.

32 A. Najjar and R. Karaman, *Expet Opin. Drug Deliv.*, 2019, **16**, 1–5.

33 Q. Meng, H. Hu, L. Zhou, Y. Zhang, B. Yu, Y. Shena and H. Cong, *Polym. Chem.*, 2019, **10**, 306–324.

34 A. G. Cheetham, R. W. Chakroun, W. Ma and H. Cui, *Chem. Soc. Rev.*, 2017, **46**, 6638–6663.

35 Y. Wang, H. Wang, Y. Chen, X. Liu, Q. Jin and J. Ji, *Colloids Surf. B Biointerfaces*, 2014, **121**, 189–195.

36 H.-L. Mao, F. Qian, S. Li, J.-W. Shen, C.-K. Ye, L. Hua, L.-Z. Zhang, D.-M. Wu, J. Lu, R.-T. Yu and H.-M. Liu, *Mol. Pharm.*, 2019, **16**, 987–994.

37 L. Zhu, D. Zhang, D. Qu, Q. Wang, X. Ma and H. Tian, *Chem. Commun.*, 2010, **46**, 2587–2589.

38 Q. Yan, J. Yuan, Z. Cai, Y. Xin, Y. Kang and Y. Yin, *J. Am. Chem. Soc.*, 2010, **132**, 9268–9270.

39 J. Lao, J. Madani, T. Puértolas, M. Álvarez, A. Hernández, R. Pazo-Cid, Á. Artal and A. A. Torres, *J. Drug Delivery*, 2013, 456409.

40 A. Shafei, W. El-Bakly, A. Sobhy, O. Wagdy, A. Reda, O. Aboelenin, A. Marzouk, K. El Habak, R. Mostafa, M. A. Ali and M. Ellithy, *Biomed. Pharmacother.*, 2017, **95**, 1209–1218.

41 O. Tacar, P. Sriamornsak and C. R. Dass, *J. Pharm. Pharmacol.*, 2013, **65**, 157–170.

42 For the experimental details, see Experimental section (S1), ESI.†

43 For characterization data, see ESI.†

44 B. S. Chhikara, D. Mandal and K. Parang, *J. Med. Chem.*, 2012, **55**, 1500–1510.

45 D. H. Altreuter, J. S. Dordick and D. S. Clark, *J. Am. Chem. Soc.*, 2002, **124**, 1871–1876.

46 B. Gidwani and A. Vyas, *BioMed Res. Int.*, 2015, 198268.

47 O. Bekers, J. H. Beijnen, M. Otagiri, A. Bult and W. J. M. Underberg, *J. Pharm. Biomed. Anal.*, 1990, **8**, 671–674.

48 H. Arima, Y. Hagiwara, F. Hirayama and K. Uekama, *J. Drug Target.*, 2008, **14**, 225–232.

49 For the FT-IR spectrum of **6**, see Fig. S9, ESI.†

50 R. Ferrazza, B. Rossi and G. Guella, *J. Phys. Chem. B*, 2014, **118**, 7147–7155.

51 H.-J. Schneider, F. Hacket, V. Rüdiger and H. Ikeda, *Chem. Rev.*, 1998, **98**, 1755–1786.

52 (*a*) For the 1H DOSY NMR spectra, see Fig. S6–S8, ESI;† ; (*b*) See section S5, ESI.†

53 X. Zhang, T. Zhang, X. Ma, Y. Wang, Y. Lu, D. Jia, X. Huang, J. Chen, Z. Xub and F. Wen, *Asian J. Pharm. Sci.*, 2019, DOI: 10.1016/j.ajps.2019.10.001.

54 Y. Kato, S. Ozawa, C. Miyamoto, Y. Maehata, A. Suzuki, T. Maeda and Y. Baba, *Canc. Cell Int.*, 2013, **13**, 89.

55 I. F. Tannock and D. Rotin, *Cancer Res.*, 1989, **49**, 4373–4384.

56 The cumulative release of DOX*HCl from the system was estimated using a dialysis technique and UV-Vis spectroscopy. For details, see subsection S1.5, ESI.†

57 M. Aliabadi, H. Shagholani and A. Yunessnia Lehi, *Int. J. Biol. Macromol.*, 2017, **98**, 287–291.

58 J. El-Ali, P. K. Sorger and K. F. Jensen, *Nature*, 2006, **442**, 403–411.

59 M. L. Coluccio, G. Perozziello, N. Malara, E. Parrotta, P. Zhang, F. Gentile, T. Limongi, P. M. Raj, G. Cuda, P. Candeloro and E. Di Fabrizio, *Microelectron. Eng.*, 2019, **208**, 14–28.

60 A. Zuchowska, K. Kwapiszewska, M. Chudy, A. Dybko and Z. Brzozka, *Electrophoresis*, 2017, **38**, 1206–1216.

61 For details on the cell-on-a-chip microfluidic system used, as well as for the details on biological assays performed, see subsection 1.6, ESI.†

62 K. Kwapiszewska, A. Michalczuk, M. Rybka, R. Kwapiszewski and Z. Brzózka, *Lab Chip*, 2014, **14**, 2096–2104.